INVARIANT CHARACTERIZING THERMALLY ACTIVATED PLASTIC FLOW

CĂTĂLIN R. PICU

Abstract. Thermal activation leads to a reduction of the flow stress below the athermal value (the zero Kelvin flow stress). The ratio between the flow stress at a given temperature and the athermal stress (at given material structure) is known as the Cottrell-Stokes ratio – a fundamental parameter describing thermal activation. This ratio is independent of strain in pure metals. This observation represents the Cottrell-Stokes law. Here it is shown that the ratio is also independent of the annealing state of the material, i.e. an invariant of the deformation and microstructure in Al alloys. A model of thermally activated dislocation motion across fields of obstacles is used to investigate the physics of the process. It is also used to discuss whether the validity of the Cottrell-Stokes law can be determined based on strain rate jump experiments and the Haasen plot, as usual in the current practice.

Key words: thermal activation, strain rate sensitivity, plastic flow, Cottrell-Stokes law, Al alloys.

1. INTRODUCTION

In 1955, Cottrell and Stokes published a seminal article on the effect of thermal activation on the plastic flow [1]. They discovered that in pure Al single crystals the ratio of the flow stress at two temperatures and same "material structure" is a function of the two temperatures at which the tests are performed and is independent of strain. This ratio is known as the Cottrell-Stokes (CS) ratio, $\sigma(T)/\sigma(T_0)$, and its strain independence is known as the CS law. An intense activity inspired by this observation followed [2–13]. With the conjecture that the CS law is valid for any two temperatures T and T_0 (provided these are low enough) and the CS ratio is a function of the difference between them, $\sigma(T)/\sigma(T_0) = f(T - T_0)$, it was proposed that testing the validity of the CS law amounts to demonstrating that $(\sigma(T_0) - \sigma(T))/\sigma(T_0)$ is independent of strain or, taking the limit of infinitesimal changes of temperature, that $\frac{1}{\sigma}\frac{\partial \sigma}{\partial T}$ is strain independent [2]. Testing these ideas requires performing experiments in which the temperature is changed rapidly at given strain. The sample is partially unloaded to

Rensselaer Polytechnic Institute, Troy, NY 12180, USA

Rev. Roum. Sci. Techn. – Méc. Appl., Tome 55, Nº 3, P. 233–242, Bucarest, 2010

avoid significant structural evolution by creep, and the temperature is modified, upon which the test continues. The temperature has to be changed fast and unloading should be kept at a minimum.

To avoid these problems, an alternative method for testing the validity of the CS law based on strain rate variation was developed. The equivalence is rooted in the Arrhenius expression for thermally activated flow [*e.g.* 14]:

$$\dot{\varepsilon} = \dot{\varepsilon}_0 \exp(-(G-(\sigma-\sigma_{ath})V)/kT) ,$$

where σ_{ath} is the athermal component of the flow stress, G is an activation energy and V is the activation volume, which implies that the functional form of the relationship between the flow stress σ and T is identical to that between σ and $\log\dot{\varepsilon}$. Hence, $\frac{1}{\sigma}\frac{\partial\sigma}{\partial T}$ may be replaced by $\frac{1}{\sigma}\frac{\partial\sigma}{\partial\log\dot{\varepsilon}}=\frac{S}{\sigma}=m$. This interpretation of the CS law requires that the strain rate sensitivity parameter m ($m=\frac{\partial\log\sigma}{\partial\log\dot{\varepsilon}}$) is strain independent. Equivalently, the strain rate sensitivity coefficient S should be proportional to the stress. These tests require performing strain rate jumps at various strains (i.e probing given "material structure" at two strain rates). In a Haasen plot (S vs. the flow stress, σ), the CS law mandates that the data points align on a line passing through the origin. This type of tests (based on strain rate jumps) was used extensively to probe the validity of the CS law.

The CS law was tested in Al single and polycrystals by Cottrell and Stokes [1] and by Basinski [2]. Cu, Ni and Ag single crystals were also studied [2, 3, 15–17]. A general agreement exists that in all these materials the CS law is valid at least in Stage I and potentially in Stage II of the deformation. Departures were observed in Stage III and at the very beginning of the deformation. Hollang *et al.* [13] have shown that the law is valid in single crystals, fine-crystalline and sub-microcrystalline Ni. It was also shown to hold in pure non-fcc materials (Cd and Zn) [7], as well as in Ni_3(Al,Hf)B intermetallics [11].

It is believed that the CS law does not hold in alloys. This is based on the observation that, as discussed extensively in the literature, the Haasen plot of alloys does not pass through the origin of the (S, σ) coordinate system. The Haasen plot of a solid solution is a curve that may have a linear segment at low stress, but intercepts the vertical axis at a positive value. As the material is annealed and precipitation begins, the intercept of the Haasen plot becomes negative. Overageing leads to a slight reduction of the slope of the plot, but the intercept remains negative. Hence, if the validity of the CS law is determined using strain rate jumps, it would be concluded that essentially all alloys do not follow the law. This is the dominant current understanding on this issue.

In this work we consider a commercial Al alloy with microstructure that can be accurately controlled throughout the entire precipitation sequence, from the solid solution to the overaged stage. Temperature variation tests (the original CS

tests) are performed and it is shown that the ratio of the flow stress at given temperature and the athermal, zero Kelvin (extrapolated) stress is independent of strain. The ratio is also identical in all stages of precipitation and equal to the ratio measured by Cottrell and Stokes [1] for pure Al single crystals. Therefore, the CS ratio $\eta(T) = \lim_{T_0 \to 0}[\sigma(T)/\sigma(T_0)]$ *is an invariant of the microstructure and depends exclusively on temperature*. Hence, this is a fundamental measure of thermal activation.

2. **EXPERIMENTAL**

The material used in this work is AA6022 supplied by Alcoa Inc. The chemical composition is 0.56 wt% Mg, 1.2 wt% Si, Cu (0.05 wt%), Mn (0.08 wt%) and residual Fe (0.12 wt%). The main alloying elements are Si and Mg. This alloy can be heat treated to obtain various precipitation states. The following procedure was used: the as received material is put in solid solution by annealing at 550 ^{o}C for 2h, quenched and rested for four hours at room temperature. In this state, which we denote as "no heat treatment" (NHT), the material is predominantly a supersaturated solid solution. Subsequently, annealing at 200^{o}C is performed for various durations. In the current tests we consider three precipitation states, obtained by annealing for 30, 90 and 150 minutes at 200^{o}C. The first is an under-aged state in which pre-β" precipitates begin to form (denoted as "under-aged" (UA)). The second state (denoted as UAp) is also under-aged, but the microstructure contains larger and less dense pre-β" precipitates. The peak-aged state (denoted as PA) is obtained after 150 min of annealing and contains a fine dispersion of β" precipitates which are fine needles aligned in the $<100>_{Al}$ directions. Therefore, the samples used in this study have significantly different microstructures, with precipitates of different types and densities. The evolution of dislocations, the dislocation structure and strain hardening are also expected to be significantly different.

Testing is performed in the following way: a prestrain ε_p is applied at room temperature (T) with a strain rate $\dot{\varepsilon}_p = 10^{-3}\text{s}^{-1}$. The sample is partially unloaded and the temperature is reduced to $T_0 < T$. Cooling is performed as fast as possible. Unloading is kept to a minimum in order to prevent structural changes. Once the temperature is equilibrated, the deformation continues at strain rate $\dot{\varepsilon}$. Unless specified otherwise, $\dot{\varepsilon} = \dot{\varepsilon}_p$. The yield stress at the current temperature $\sigma(\varepsilon_p, \dot{\varepsilon}, T_0)$ is recorded. Multiple samples are prepared under the same conditions and reloaded at lower and lower temperatures, T_0, down to a minimum temperature of 98 ^{o}K. The temperature dependence of $\sigma(\varepsilon_p, \dot{\varepsilon}, T_0)$ is fitted accurately by an exponential (Fig. 1).

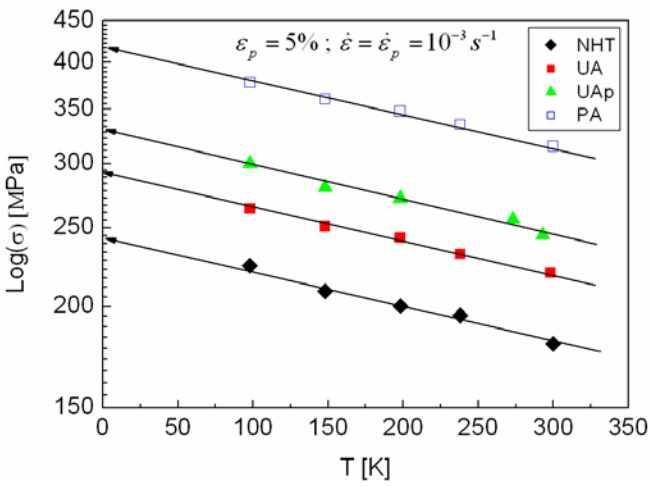

Fig. 1 – Flow stress at various temperatures and constant structure for NHT, UA, UAp and PA samples. The lines are exponential fits and the arrows indicate the extrapolated values of the flow stress (athermal limit) at 0^{o}K.

The CS ratio is computed as $\eta(T) = \lim_{T_0 \to 0} [\sigma(\varepsilon_p, \dot{\varepsilon}, T) / \sigma(\varepsilon_p, \dot{\varepsilon}, T_0)]$, *i.e.* the ratio of the flow stress at the given prestrain and temperature and the effective flow stress at 0^{o}K corresponding to the *same internal structure* of the material. The internal structure is defined by the prestraining conditions.

It must be noted that the extrapolated value $\sigma(\varepsilon_p, \dot{\varepsilon}, 0)$ is not the flow stress one would measure if tests could be performed at $0\ ^{o}$K. At temperatures below approximately 50^{o}K, quantum effects begin to dominate and the motion of dislocations is different from what is observed at higher temperatures. However, it is a value consistent with the material behaviour at higher (but sub-ambient) temperatures.

3. **RESULTS**

The central results of this work are presented in Fig. 2. Figure 2a shows the ratio η measured at 5% prestrain for all materials considered in this study. It is seen that, although the microstructures of these alloys are very different, η takes values in a narrow range between 0.73 and 0.75.

Figure 2b shows the variation of ratio η with strain for all alloys considered. As above, this quantity is independent of strain and identical in all systems. The η values vary again in a narrow range in the vicinity of 0.75. It should be observed that 0.75 is also the value measured by Cottrell and Stokes for pure Al single crystals!

The data in Fig. 2b indicate that the ratio is independent of the dislocation microstructure (which is controlled primarily by the applied plastic (pre)strain), while the results in Fig. 2a show that the precipitation microstructure has also no effect on η. This renders η a function of temperature only, as already implied by the relations written above. It turns out that η is an invariant of the microstructure, at least in this material system.

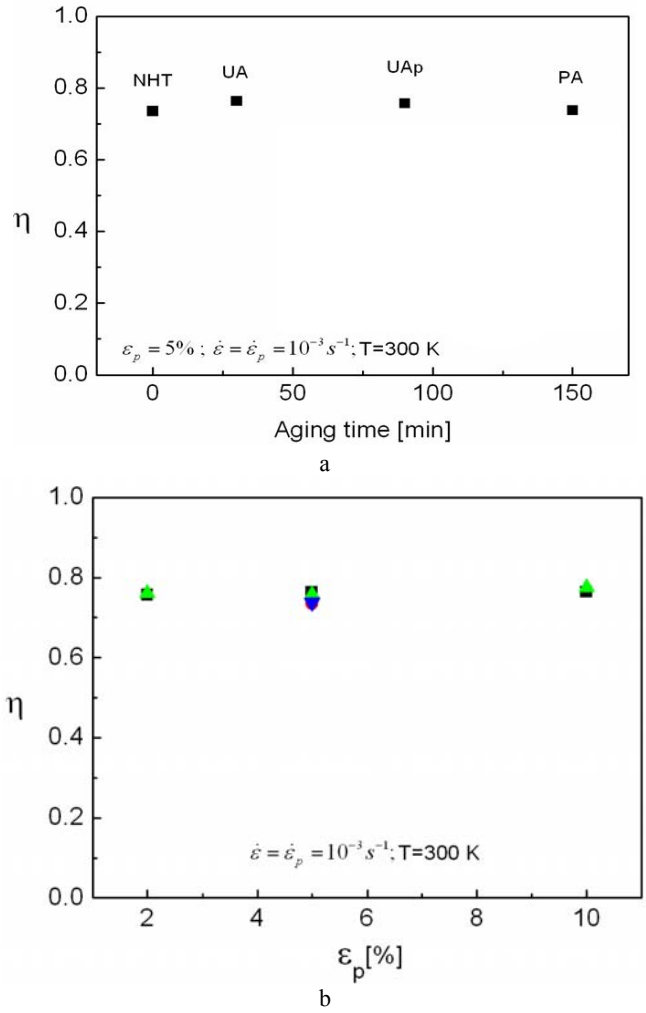

Fig. 2 – Values of ratio η for: a) the four annealing states considered;
b) as a function of strain (pre-strain) for all alloys considered.

It is interesting to investigate how η changes with temperature. The relevant data is shown in Fig. 3. The ratio η decreases monotonically with increasing temperature, as expected.

Let us use a model of thermally activated glide of dislocations across field of obstacles in their glide plane to gain insight into some of the phenomenology described above. The model was described extensively in other publications [18, 19]. For completeness, only the essential features are discussed here.

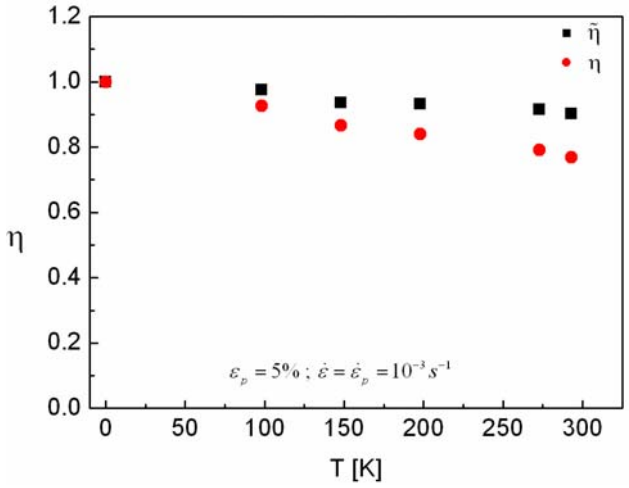

Fig. 3 – Variation of ratio η with the temperature. The squares represent the normalized ratio $\tilde{\eta}(T) = \lim_{T_0 \to 0} [(\sigma(\varepsilon_p, \dot{\varepsilon}, T) E(T_0)) / (\sigma(\varepsilon_p, \dot{\varepsilon}, T_0) E(T))]$.

The dislocations are represented as flexible strings of line tension $\Gamma = 1/2 Gb^2$ (G is the shear modulus and b is the Burgers vector length). Randomly distributed obstacles are placed in the glide plane and the average distance between them is $l_c = 1/\sqrt{\rho}$, where ρ is the obstacle number density.

Under the action of the shear stress τ, a segment of length l_c pinned by two obstacles bows out into an arc of dimensionless radius $r^* = 1/2\tau^*$. The applied shear stress τ^* is normalized by the Orowan stress Gb/l_c, $\tau^* = \dfrac{\tau l_c}{Gb}$. The force acting on the respective obstacles is $F = 2\Gamma \cos\left(\dfrac{\theta}{2}\right)$, where θ is the angle made by the two branches of the dislocation impinging against the obstacle. Let us use the non-dimensional form $f = \dfrac{F}{2\Gamma} = \cos\left(\dfrac{\theta}{2}\right)$ for the force. The obstacle strength is defined as the maximum allowed force $f_c = \cos(\theta_c / 2)$.

The 0°K resolved shear stress τ_0^*, at which dislocations glide through in absence of thermal activation, has been evaluated theoretically (Friedel's result

[20] indicates $\tau_0^* = f_c^{3/2}$) and numerically. Once the applied stress is normalized by τ_0^*, the CS ratio results: $\eta = \tau^*/\tau_0^*$. η is the control parameter of all simulations.

The obstacle-dislocation interaction is described in terms of an activation energy $\Delta G = 2\Gamma d\Delta G^*$, where d is a characteristic interaction range. Γd becomes the unit of energy of the problem. The normalized activation energy is written $\Delta G^* = \beta f_c(1-f^*)^n$, with $f^* = f/f_c$ being the reduced dislocation-obstacle interaction force. ΔG^* depends on the obstacle nature but decreases monotonically with f^*. The power $n = 2$ is considered in all simulations.

The per-attempt probability that the dislocation overcomes an obstacle is given by the Arrhenius form $p = \exp\left(-\alpha\Delta G^*\right)$, where $\frac{1}{\alpha} = \frac{kT}{2\Gamma d}$ is the dimensionless temperature. A stable configuration is obtained when two conditions are fulfilled at all obstacles in contact with the dislocation: the dislocation bows out into an arc of circle of radius smaller than the critical one (no Orowan looping) and the force acting on all obstacles is smaller than f_c.

The thermally activated motion of a dislocation across arrays composed from obstacles of multiple types was studied. Obstacles with normalized strength f_c = = 0.1, 0.3, 0.5, 0.7 and 0.9 were considered, at relative concentrations $\mathbf{c} = \{c_1, c_2, c_3, c_4, c_5\}$, with $\sum_{i=1}^{5} c_i = 1$. Vector $\mathbf{c}$ is modified from simulation to simulation. We seek the admissible values of η at given temperature, α, and imposed strain rate (mean dislocation velocity, v^*) as $\mathbf{c}$ changes. The results are shown in Fig. 4, where η vs. $\log(v^*)$ data are presented for 15 obstacle populations, $\mathbf{c}$. The maximum normalized velocity that can be reached in this model is $v^* = 1$. This happens when motion is fully stress activated, in the athermal limit (note that $\eta = 1$ is a critical point for the system). At smaller velocities and in presence of thermal activation, each $\mathbf{c}$ corresponds to a different η. However, it is observed that the range of η at given v^* becomes narrower as the critical point is approached. In other words, if the deformation rate is large enough, the system appears to "select" a value of η. Ratio η becomes more sensitive to the composition $\mathbf{c}$ when the system is deformed at small rates.

Let us use the model to investigate the relationship between the CS law and the Haasen plot. As discussed above, the Haasen plot (the strain rate sensitivity coefficient S vs. the flow stress, σ) is used to determine whether the CS law applies in a given material system. S being proportional to σ indicates that the law applies and η is independent of strain.

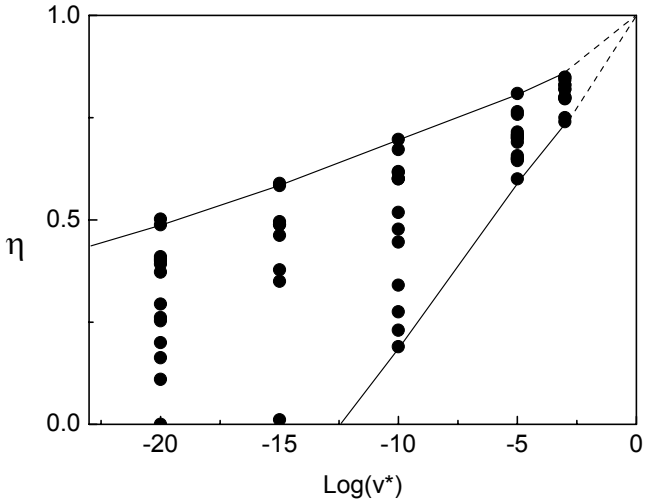

Fig. 4 – Relation between η and the dislocation velocity at imposed temperature and η, and for many heterogeneous populations of obstacles of various compositions, **c**.

Let us consider systems with various compositions **c** loaded at $\eta = 0.75$. By keeping η constant, the CS law is imposed. In experiments, as the material deforms, **c** and the obstacle density ρ change, but η remains constant. Our objective is to determine the effect of these two parameters on the Haasen plot, at constant η. To this end, nineteen compositions **c** are considered and the strain rate sensitivity coefficient *S,* as well as the flow stress, are determined numerically. The open data points in Fig. 5 (Haasen plot) correspond to these configurations at normalized density $\rho = 1$. The five filled data points (labeled A, B, C, D and E) correspond to homogeneous systems in which only one type of obstacle is present. The composition **c** is shown for several of these systems in the form of histograms. These are arranged along lines MN and MPQ, with MN going through the origin, and MPQ having a positive intercept with the vertical axis. If the composition **c** is held constant and the density increases, the resulting Haasen plot is a straight line going though the origin. The arrows starting from points M, P and Q in Fig. 2 show how the respective point moves in the S-τ^* field when the density increases while **c** is kept constant. In principle, any path in the $\eta = \tau^*/\tau_0^*$ plane (Fig. 5) is available, including curves with positive, zero or negative intercepts.

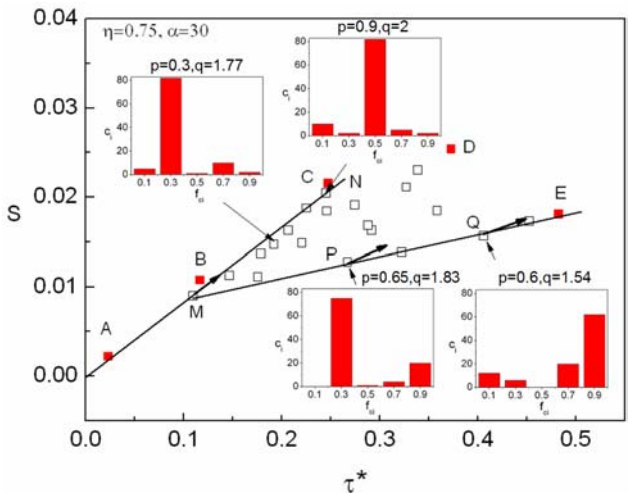

Fig. 5 – *S*-τ∗ (Haaasen) plot for nineteen heterogeneous systems (open data points) with different **c** and same density ($\rho = 1$), and for five homogeneous systems (filled symbols) with 100% obstacles with $f_c = 0.1$ (point A), 0.3 (point B), 0.5 (point C), 0.7 (point D), and 0.9 (point E) and $\rho = 1$. The CS ratio is identical for all systems, $\eta = 0.75$. The histograms show the composition **c** for several configurations.

This demonstrates that even though η is held constant, the Haasen plot may have multiple shapes and therefore, using the Haasen plot to determine the validity of the CS law is not always mandated.

4. **CONCLUSIONS**

Experimental and numerical data presented in this article indicate that:

- The Cottrell-Stokes ratio η is an invariant of the microstructure and depends exclusively on temperature. Therefore, this parameter appears to be a fundamental quantity describing thermal activation.
- A simple model of thermally activated dislocation motion across fields of obstacles indicates that the range in which the ratio can take values decreases as the deformation strain rate increases. This suggests an alternative explanation for the CS law.
- Using the Haasen plot to determine whether the CS law applies in a certain material system may lead to incorrect conclusions. CS-type experiments involving temperature changes, rather than strain rate jump experiments, must be performed to determine the validity of the law.

Acknowledgements. Several people contributed to various aspects of this work: Dr. G. Vincze and Prof. J. Gracio from University of Aveiro, Aveiro, Portugal, contributed to the

experimental work, while Dr. R. Li performed some of the numerical simulations. The author also acknowledges the support from the US National Science Foundation through grant CMS-0502891.

Received on July 10, 2010

REFERENCES

1. COTRELL, A.H., STOKES, R.J., *Effects of temperature on the plastic properties of aluminum crystals*, Proc. R. Soc. London, **A233**, pp. 17-34, 1955.
2. BASINSKI, Z.S., *Thermally activated glide in FCC metals and its application to the theory of strain hardening*, Phil. Mag., **4**, pp. 393-432, 1959.
3. MECKING, H., LUCKE, K., *Die Bestimmung des Aktivierungsvolumens durch Wechsel der Dehngeschwin insbesondere an Silbereinkristallen*, Mater. Sci. Eng., **1**, pp. 342-348, 1967.
4. BASINSKI, Z.S., *Forest hardening in FCC metals*, Scripta Metall., **8**, pp. 1301-1308, 1974.
5. BASINSKI, Z.S., FOXALL, R.A., PASCUAL, R., *Stress equivalence of solution hardening*, Scripta Metall., **6**, pp. 807-814, 1972.
6. ZEYFANG, R., BUCK, O., SEEGER, A., *Thermally activated plastic deformation of high purity Cu single crystals*, Phys. Stat. Sol., **B61**, pp. 551-561, 1974.
7. WIELKE, B., TIKVIC, W., SCHOECK, G., *Cottrell-Stokes law in Cd and Zn*, Phys. Stat. Sol., **A40**, pp. 271-277, 1977.
8. MECKING, H., KOCKS, U.F., *Kinetics of flow and strain-hardening*, Acta Metall., **29**, pp. 1865-1885, 1981.
9. SAIMOTO, S., SANG, H., *A re-examination of the Cottrell-Stokes relation based on precision measurements of the activation volume*, Acta Metall., **31**, pp. 1873-1881, 1983.
10. BOCHNIAK, W., *The Cottrell-Stokes law for FCC single crystals*, Acta Metall. Mater., **41**, pp. 3133-3140, 1993.
11. EZZ, S.S., SUN, Y.Q., HIRSCH, P.B., *Strain rate dependence of the flow stress on work hardening of γ'*, Mat. Sci. Eng., **A192/193**, pp. 45-52, 1995.
12. KRUML, T., CODDET, O., MARTIN, J.L., *The investigation of internal stress fields by stress reduction experiments*, Mat. Sci. Eng., **A387-389**, pp. 72-75, 2004.
13. HOLLANG, L., HIECKMANN, E., BRUNNER, D., HOLSTE, C., SKROTZKI, W., *Scaling effects in plasticity of Ni*, Mat. Sci. Eng., **A424**, pp. 138-153, 2006.
14. SEEGER, A., *The generation of lattice defects by moving dislocations, and its application to the temperature dependence of the flow-stress of fcc crystals*, Phil. Mag., **46**, pp. 1194-1198, 1955.
15. ADAMS, M.A., COTTRELL, A.H., *Effect of temperature on the flow stress of work-hardened copper crystals*, Phil. Mag., **46**, pp. 1187-1193, 1955.
16. BULLEN, F.P., COUSLAND, S.M., *Energy levels of electron and hole traps in the band gap of doped anthracene crystals*, Phys. Stat. Sol., **27**, pp. 501-508, 1968.
17. HAASEN, P., *Plastic deformation of nickel single crystals at low temperatures*, Phil. Mag., **3**, p. 384, 1958.
18. XU, Z., PICU, R.C., *Thermally activated motion of dislocations in fields of obstacles: the effect of obstacle distribution*, Phys. Rev., **B76**, pp. 094112(1)-(8), 2007.
19. PICU, R.C., LI, R., XU, Z., *Strain rate sensitivity of thermally activated dislocation motion across fields of obstacles of different kind*, Mat. Sci. Eng., **A502**, pp. 164-171, 2009.
20. FREIDEL, J., *Dislocations,* Addison-Wesley, Reading, MA, 1967.